

Evidence for a High Carbon Abundance in the Local Interstellar Cloud

Jonathan D. Slavin¹ and Priscilla C. Frisch²

ABSTRACT

The nature of the Local Interstellar Cloud (LIC) is highly constrained by the combination of *in situ* heliospheric and line-of-sight data towards nearby stars. We present a new interpretation of the LIC components of the absorption line data towards ϵ CMa, based on recent atomic data that include new rates for the Mg^+ to Mg^0 dielectronic recombination rate, and using *in situ* measurements of the temperature and density of neutral helium inside of the heliosphere. With these data we are able to place interesting limits on the gas phase abundance of carbon in the LIC. If the C/S abundance ratio is solar, ~ 20 , then no simultaneous solution exists for the $N(\text{Mg I})$, $N(\text{Mg II})$, $N(\text{C II})$ and $N(\text{C II}^*)$ data. The combined column density and *in situ* data favor an abundance ratio $A_{\text{C}}/A_{\text{S}} = 47_{-26}^{+22}$.

We find that the most probable gas phase C abundance is in the range 400 to 800 ppm with a lower limit of ~ 330 . We speculate that such a supersolar abundance could have come to be present in the LIC via destruction of decoupled dust grains. Similar enhanced C/H ratios are seen in very low column density material, $N(\text{H}) < 10^{19} \text{ cm}^{-2}$, towards several nearby stars.

Subject headings: ISM: clouds — ISM: abundances — ultraviolet: ISM

1. Introduction

The interstellar cloud that surrounds our solar system, the Local Interstellar Cloud (LIC), is a tiny, radius $\lesssim 1$ pc, low density interstellar cloud that has been detected in absorption lines towards many towards nearby stars (e.g., McClintock et al. 1978; Bruhweiler 1984; Genova et al. 1990; Lallement & Ferlet 1997; Hébrard et al. 1999; Gry & Jenkins 2001; Wood & Linsky 1997). The cloud is partially ionized, $\sim 20 - 40\%$, apparently due to the low intensity, relatively hard ionizing radiation field (Slavin & Frisch 2002; Frisch & Slavin 2003, hereafter SF02). Direct observations of interstellar He^0 which penetrates the heliosphere gives us tight constraints on its temperature and density: $T = 6300 \pm 340$ K, $n(\text{He}^0) = 0.015 \pm 0.0015 \text{ cm}^{-3}$ (Witte 2004; Möbius et al. 2004).

The star ϵ CMa (HD 52089) is located in the downwind direction of the flow of ISM past the Sun ($\ell = 239.8^\circ$, $b = -11.3^\circ$, $d = 132$ pc). The absorption line data set for the line of sight

¹Harvard-Smithsonian Center for Astrophysics, 60 Garden Street, MS 83, Cambridge, MA 02138

²University of Chicago, Department of Astronomy and Astrophysics, 5460 S. Ellis Avenue, Chicago, IL 60637

towards ϵ CMa is particularly complete (Gry & Jenkins 2001, hereafter GJ). Using this dataset, in particular the ratios $N(\text{Mg II})/N(\text{Mg I})$ and $N(\text{C II}^*)/N(\text{C II})$, GJ put constraints on the electron density, $n(e)$, and temperature of the LIC and of the other clouds seen in this line of sight. As we discuss, their method involved assuming a gas phase abundance ratio for C/S of 20, appropriate to Solar abundances. However, we show that when updated atomic rates are used for the Mg^+ recombination coefficient, in particular for dielectronic recombination, this solution becomes no longer viable. This leads us to the conclusion that C has a supersolar abundance in the LIC, $A_{\text{C}} = 400 - 800$ ppm (parts per million). This result, which is consistent with detailed models of the photoionization of the LIC (Slavin & Frisch 2006, hereafter SF06), then allows for a solution for $n(e)$ which is consistent with all other data. High carbon abundances are also seen towards several other stars that sample the LIC.

2. Data

GJ presented data obtained with the GHRS on HST, and IMAPS on ORFEUS, of the absorption lines from a number of ions observed towards ϵ CMa, including Mg I, Mg II, C II, C II* and S II. Multiple velocity components are seen in this line of sight, but here we concentrate on the LIC component, referred to as component 1 by GJ, at a heliocentric velocity of ~ 17 km s $^{-1}$. The derived column densities, along with the errors estimated by GJ, are listed in Table 1. GJ determined a lower limit on $N(\text{C II})$ directly from the observed absorption line, but needed to rely on an assumption for the abundance ratio of C to S to derive the upper limit on the column density because of the degree of saturation of the 1335 Å C II line. From these data, using pre-1982 atomic rate constants, GJ obtained $T = 5700 - 8200$ K and $n(e) = 0.08 - 0.17$ cm $^{-3}$.

For the LIC we have the additional constraint given by *in situ* observations of the temperature of inflowing He 0 determined from direct measurements inside of the solar system by the GAS instrument on the Ulysses space craft, $T = 6300 \pm 340$ K Witte (2004, see also Möbius et al. 2004). Because of the small column density of the LIC along the ϵ CMa line of sight, $N(\text{H I}) \approx (3 - 5) \times 10^{17}$ cm $^{-2}$, the gas temperature is not expected to vary greatly along the line of sight. In our photoionization models in which we use a realistic ionizing radiation field (SF02, SF06), the typical total variation in temperature is $\sim 10\%$. We note that if GJ had required consistency with the LIC temperature in their analysis, their minimum electron density would have increased to $n(e) \sim 0.11$ cm $^{-3}$ (up from 0.08 cm $^{-3}$).

3. Mg Ionization

In ionization equilibrium the density ratio of Mg^+/Mg^0 is determined by

$$[\Gamma(\text{Mg}^0) + C^{\text{CT}}(\text{Mg}^0)n(\text{H}^+)] n(\text{Mg}^0) = \alpha(\text{Mg}^+) n(e) n(\text{Mg}^+), \quad (1)$$

where $\Gamma(\text{Mg}^0)$ is the photoionization rate, $C^{\text{CT}}(\text{Mg}^0)$ is the charge transfer ionization rate for Mg^0 with H^+ , $\alpha(\text{Mg}^+)$ is the total Mg^+ recombination coefficient (including both radiative and dielectronic recombination), and $n(e)$ is the electron density. The dominant contribution to the photoionization rate for Mg^0 is the FUV background, which comes mostly from A and B stars. The spectrum and flux of the background has been estimated by a number of authors. We choose to use the results of Gondhalekar et al. (1980) because they make use of the TD-1 observations, which remain the best direct measurements of the background from stars and includes the whole sky. This is important because the sky is extremely anisotropic in the FUV and other observations have covered only brighter than average portions of the sky. Integrating the Gondhalekar et al. (1980) spectrum over the Mg^0 photoionization cross section leads to a value of $\Gamma(\text{Mg}^0) = 4.5 \times 10^{-11} \text{ s}^{-1}$. The uncertainty of the FUV spectrum is estimated by Gondhalekar et al. (1980) to be 25%. The Mg^0 photoionization cross section we use comes from Verner et al. (1996) and is based on results from the Opacity Project. Our value for the photoionization rate is significantly below the value $6.1 \times 10^{-11} \text{ s}^{-1}$ used by GJ, which was based on estimates by Jura (1974) and Mathis et al. (1983). The rate of charge transfer ionization of Mg^0 is taken from the fit provided in Kingdon & Ferland (1996), which was based on data from Allan et al. (1988), and gives $C^{\text{CT}}(\text{Mg}^0) = 6.5 \times 10^{-11} \text{ cm}^3 \text{ s}^{-1}$ at $T = 6300 \text{ K}$.

The recombination rates, both dielectronic and radiative, are taken from new calculations. The radiative rates we use are recently calculated by Badnell¹ using the AUTOSTRUCTURE code. These rates are considerably larger than those calculated by Aldrovandi & Péquignot (1973). We use the dielectronic recombination rates calculated by this group as well (Altun et al. 2006), which are also larger than the older combined low temperature (Nussbaumer & Storey 1986) and high temperature (Burgess 1965) rates. The resulting total Mg^+ recombination rate for the LIC temperature range is $\alpha(\text{Mg}^+) = 1.71_{-0.34}^{+0.43} \times 10^{-12} \text{ cm}^3 \text{ s}^{-1}$. As a result of the higher rates, the electron density inferred for a given observed ratio $N(\text{Mg II})/N(\text{Mg I})$ is considerably lower than if the older rates had been used. It should be emphasized that there are considerable uncertainties in these theoretical dielectronic recombination rates. The low temperature ($< 10^4 \text{ K}$) dielectronic recombination rates in particular need to be confirmed by laboratory measurements and further theoretical calculations. Since we do not have any way of estimating the magnitude of the uncertainties in the rates we do not include the uncertainties in our numerical results and plots. Some comfort may be taken from the fact that other recently calculated rates (Gu 2004) are within $\sim 30\%$ of the Altun et al. (2006) results for temperatures of interest, though this does not guarantee their accuracy to that level.

To use equation (1) to solve for the electron density, one needs to know $n(\text{H}^+)$. Based on our ionization models (SF02) and the observation that $N(\text{H I})/N(\text{He I}) \gtrsim 12$ (Dupuis et al. 1995) in the local ISM, we assume that $n(\text{H}^+) = 0.9n(e)$. This should be good to about 10% and in any case the charge transfer term is small compared with the recombination term in the equation for

¹<http://amdpp.phys.strath.ac.uk/tamoc/DATA/RR/>

the electron density.

4. C⁺ Fine Structure Excitation

The ratio of C⁺ ions in the excited $J = 3/2$ fine structure level of the ground state to that in the $J = 1/2$ level is another measure of $n(e)$. The equilibrium populations of the two states are given by

$$\frac{n(\text{C}^{+*})}{n(\text{C}^+)} = \frac{\gamma_{12}n(e) + \gamma_{12}^H n(\text{H}^0)}{A_{21} + \gamma_{21}n(e) + \gamma_{21}^H n(\text{H}^0)}, \quad (2)$$

where $A_{21} = 2.29 \times 10^{-6} \text{ s}^{-1}$ is the radiative decay probability, and γ_{12} and γ_{21} are the excitation and de-excitation coefficients respectively for collisions with electrons and γ_{12}^H and γ_{21}^H are the corresponding coefficients for excitation by neutral H. The electron collisional excitation coefficient is $\gamma_{12} = \frac{8.63 \times 10^{-6}}{g_1 T^{1/2}} \Omega_{12} \exp(-\frac{E_{12}}{kT})$, where g_1 is the statistical weight ($= 2$) of the lower level, Ω_{12} is the collision strength and E_{12} is the excitation energy (see, e.g. Spitzer 1978). For partially ionized warm gas such as in the LIC the excitation of C⁺ by neutral H is small compared with excitation by electrons but for completeness we include it using rates from Keenan et al. (1986) and assuming a H⁰ density of 0.2 cm^{-3} , which should be roughly correct. We use the collision strength from Blum & Pradhan (1992), which is substantially smaller ($\Omega_{12} \approx 2.0$ at $T = 6300 \text{ K}$) than the Hayes & Nussbaumer (1984) value used by GJ (2.81). This smaller value is consistent within 5% with recent calculations by Wilson & Bell (2002). A smaller value for Ω_{12} leads to a larger value for $n(e)$ estimated from $N(\text{C II}^*)/N(\text{C II})$. For $T = 6300 \text{ K}$, $\gamma_{12} = 1.07 \times 10^{-7} \text{ cm}^3 \text{ s}^{-1}$.

5. Results

Following GJ, we determine $n(e)$ from the overlap region that is consistent with both $N(\text{C II}^*)/N(\text{C II})$ and $N(\text{Mg I})/N(\text{Mg II})$. The updated atomic data we use leads to significantly different values from those found by GJ. Figure 1 illustrates the allowed region for $n(e)$ as a function of T , based on equations (2) and (1) and the LIC temperature constraints. The allowed range of $n(e)$ is much smaller than found previously primarily because of the limits on the temperature provided by the *in situ* observations. As can be seen from equation (2), the lower limit on $n(e)$ from $N(\text{C II}^*)/N(\text{C II})$ comes from the lower limit on the observed ratio. In the figure the dashed line, labeled “C II*/C II (C/S = 20)”, uses an upper limit on $N(\text{C II})$ derived from taking the upper limit on $N(\text{S II})$ and an assumed C/S abundance ratio of 20. Clearly this value does not allow for a solution consistent with the Mg ion column densities and LIC temperature. The lower curve corresponds to a $N(\text{C II})$ upper limit derived from assuming a C/S abundance ratio of 40, and allows a solution with the resulting limits of $n(e) = 0.050 - 0.104 \text{ cm}^{-3}$ when T is limited by the *in situ* He data. While C/S need not be as high as 40 to find an allowed region in the plot, a value of $\gtrsim 21$ is required.

An alternative method of placing constraints on the C/S abundance ratio is to use $N(\text{Mg I})$,

$N(\text{Mg II})$ and T to derive $n(e)$, and then $N(\text{C II}^*)$ and $N(\text{S II})$ to find A_C/A_S ($A_C \equiv \text{C/H}$ and $A_S \equiv \text{S/H}$). Combining equations (1) and (2), we find

$$\frac{A_C}{A_S} = \frac{A_{21} + \gamma_{21}n(e)}{\gamma_{12}n(e)} \frac{N(\text{C II}^*)}{N(\text{S II})} \quad (3)$$

where $n(e)$ is derived via equation (1). Observations with reasonable uncertainties exist for all of the quantities needed to determine A_C/A_S . A straightforward propagation of errors approach yields $A_C/A_S = 46.8 \pm 25.7$ (including uncertainties in the temperature and its effect on the rate coefficients). The uncertainties involved in the expressions contribute in nonlinear ways, however, so we have in addition carried out a Monte Carlo simulation to estimate the errors. To do this we have used the $1\text{-}\sigma$ reported errors for the observed quantities, assumed normally distributed errors and calculated the resulting A_C/A_S from equation 3 for many trials. The resulting probability distribution is very asymmetric with a long tail to high values of A_C/A_S . The result is $A_C/A_S = 46.8_{-26.2}^{+22.0}$, where the error limits are those that contain 68.3% of the probability surrounding the peak in the distribution. The peak of the probability distribution function is at 37.2 and the mean (expected value) is 58.5. Alternatively we may state that the $A_C/A_S > 21$ with 95.45% confidence or $A_C/A_S > 39$ with 68.3% confidence (note that the long tail to high values causes this one-sided limit to exceed the value at the peak of the probability distribution). The high-value tail is a standard result for the ratio of two values in which the errors for each quantity are a relatively large fraction of the quantity. The inclusion of the uncertainty in the Mg^0 photoionization rate broadens the uncertainty range in $n(e)$ beyond that indicated in Figure 1. The Mg ionization calculations also yield the probability distribution for electron density for which we find $n(e) = 0.064_{-0.036}^{+0.021}$, where again we report the limits that enclose 68.3% of the probability. For $n(e)$ the peak is at 0.052 cm^{-3} and the expected value is 0.067 cm^{-3} .

Determinations of the electron density for the LIC using independent sets of data, combined with models, lead Izmodenov et al. (2003), to find $n(e) = 0.07 \pm 0.02$. Similar calculations by Gloeckler & Geiss (2004), but with somewhat different assumptions gave $n(e) = 0.049 \pm 0.016$.

Another approach for evaluating the C abundance, that is separate from the S abundance, uses only the more reliable $N(\text{C II}^*)$ data. GJ placed limits on $N(\text{H I})$ and $N(\text{H}_{\text{tot}})$ using several assumptions. Using the fact that the ionization of O and H are tightly coupled by charge transfer (Field & Steigman 1971), observations of O I and an assumed gas phase abundance of 316 ppm, they find $N(\text{H I}) = 4.4_{-0.6}^{+1.6} \times 10^{17} \text{ cm}^{-3}$. A recent determination of O/H in the Local Bubble (Oliveira et al. 2005, also see André et al. (2003)) gives a value of 345 ± 19 ppm, which leads to a somewhat smaller total H I column density, $N(\text{H I}) = 4.0_{-0.6}^{+1.5} \times 10^{17} \text{ cm}^{-3}$.

The ionization fraction of H in the LIC can be estimated in various ways. Using just the directly measured EUVE flux from stars, a lower limit of $X(\text{H}^+) \geq 0.15$ can be determined. This flux is inadequate to explain the high He ionization fraction relative to H found from nearby white

dwarf stars, however.² Our models for the ionization of the LIC, which include the diffuse soft X-ray background as an ionization source and a contribution from radiation generated in an evaporative boundary between the LIC and the hot gas of the Local Bubble, predict ionization fractions of 22 – 36%. For our best new models we find total H columns ranging from $4.1 - 5.5 \times 10^{17}$. While we cannot place firm upper limits on the H ion fraction, it appears unlikely that it significantly exceeds 40% unless some additional unknown ionizing source is present or the cloud is out of photoionization equilibrium (see discussion below). Combining our H ionization fraction limits with the H I column determination leads to $N(\text{H}_{\text{tot}}) \approx 5.6_{-1.2}^{+3.0} \times 10^{17} \text{ cm}^{-2}$. This value yields a value for the S abundance of $A_{\text{S}} \sim 15$ ppm, with 50% uncertainties, in agreement with solar values of 12.3 – 15.5 (Asplund et al. 2005, AGS).

We can express the C abundance as a function of the observed value of $N(\text{C II}^*)$ as,

$$A_{\text{C}} = \frac{N(\text{C II}^*)}{N(\text{H}_{\text{tot}})} \frac{A_{21}}{\gamma_{12}n(e)} = \left(\frac{N(\text{C II}^*)}{1.3 \times 10^{12} \text{ cm}^{-2}} \right) \left(\frac{5 \times 10^{17} \text{ cm}^{-2}}{N(\text{H}_{\text{tot}})} \right) \left(\frac{0.08 \text{ cm}^{-3}}{n(e)} \right) 710 \text{ ppm} \quad (4)$$

where we have left out the less important terms for collisional de-excitation and excitation by H^0 . This expression makes it clear that the C abundance in the LIC is quite high unless $N(\text{C II}^*)$ is at the low end of its range while $N(\text{H}_{\text{tot}})$ and $n(e)$ are the high ends of theirs. In this expression $n(e)$ should be the line of sight averaged value, which is highest at the cloud edge and decreases inward on the line of sight. For our models we find that the expression leads to about an 8% overestimate for A_{C} when $n(e)$ is interpreted as the electron density at the position of the heliosphere. If we take an upper limit on $n(e) = 0.09 \text{ cm}^{-3}$, consistent with our derivation above, and an upper limit of $N(\text{H}_{\text{tot}}) = 8 \times 10^{17} \text{ cm}^{-2}$, and the lower limit of $N(\text{C II}^*) = 1.1 \times 10^{12} \text{ cm}^{-2}$ we get 334 ppm as a lower limit on the C abundance. This lower limit is consistent with the solar abundance from Grevesse & Sauval (1998), but not with the more recent results of AGS. Using a value of $N(\text{H}_{\text{tot}})$ as high as 8×10^{17} implies a S abundance of $A_{\text{S}} \lesssim 13$ ppm to be consistent with the observed upper limit for $N(\text{S II})$. Sulfur is expected to have little to no depletion in warm clouds (see e.g., Welty et al. 1999), and a solar abundance of 13.8 ppm is found by AGS.

6. Discussion

An implicit assumption in our analysis for the electron density is photoionization equilibrium. The timescale for Mg I ionization is very short, $< 10^3$ years, while the recombination timescale for Mg II is considerably longer $\sim 3 \times 10^5$ yr. The most likely scenario for the cloud to be out of photoionization equilibrium is that it is recombining and cooling from a previously heated (e.g., shocked) state (see Lyu & Bruhweiler 1996). In that case the electron density we infer would be an underestimate. This would both lower the inferred value of $A_{\text{C}}/A_{\text{S}}$ and the C abundance. However,

²For instance, the nearby white dwarf stars GD71 and HZ43 have $\chi(\text{He}) = \text{He II}/(\text{He I} + \text{He II}) = 0.31$, and 0.38 respectively (Wolff et al. 1999, and references therein).

Jenkins et al. (2000) argue, based on the relative column densities of Ar I and H I in the LIC, that photoionization dominates the ionization rather than the collisional processes that should dominate in cooling and recombining gas. It remains to be seen whether or not a non-equilibrium model could be found that would be consistent with the Ar I data as well as all the other column density data for the LIC and the *in situ* data on He⁰. We intend to explore this possibility in the future.

Observations of low column density, $N(\text{H}) < 10^{19} \text{ cm}^{-2}$, ISM towards other nearby stars, are consistent with our conclusion of supersolar C abundances. Using N I+N II as a proxy for the total H column and the AGS Solar abundance for N for the lines of sight towards Capella, WD 1254+223, WD 1314+293, and WD 1634-573 yields $A_{\text{C}} \sim 340$ ppm, with a range 83 – 550 (see data in Wood et al. 2002; Lehner et al. 2003; Oliveira et al. 2005; Kruk et al. 2002). Three of these stars show $A_{\text{C}} > 333$ ppm.

7. Conclusions

We have shown that using updated atomic data and the *in situ* data on the temperature of the gas in the LIC, we can put interesting constraints on the C abundance in the LIC. Unless a number of observed or inferred data values are at the far ends of their uncertainty ranges, it appears that C is not only undepleted in the LIC, but has an abundance of $A_{\text{C}} \approx 400 - 800$ ppm, considerably larger than the solar value. In addition, the ratio of C to S abundance appears to be necessarily larger than the solar ratio of ~ 20 with values in the range of 40 – 50 favored by the constraints on $n(e)$ in the LIC. We speculate that this supersolar abundance of C, if it truly exists, may be indicative of a local enhancement in dust in the past. In this picture the gas phase C abundance was enhanced by the passage of an interstellar shock that destroyed the carbon bearing grains more effectively than other, e.g. silicate, grains. This could be related to the unusual dust size distribution in the LIC as indicated by Ulysses observations of large grains penetrating into the heliosphere (Gruen et al. 1994; Frisch et al. 1999).

Further investigations into the C abundance in the LIC should be undertaken to confirm our findings, especially studies of other lines of sight that show the LIC velocity component in the absorption lines of C, S, Mg and other elements. The LIC is the best observed low density interstellar cloud and thus can provide us with valuable information on this phase of the interstellar medium. The C abundance and its evolution in the warm diffuse ISM has many implications for the nature of interstellar dust and metallicity in the Galaxy.

This research was supported by NASA grants NAG5-12571 and NAG5-13107. The authors thank Daniel Savin and Gary Ferland for very helpful discussions and the anonymous referee who helped improve the clarity of the presentation.

REFERENCES

- Aldrovandi, S. M. V. & Péquignot, D. 1973, *A&A*, 25, 137
- Allan, R. J., Clegg, R. E. S., Dickinson, A. S., & Flower, D. R. 1988, *MNRAS*, 235, 1245
- Altun, Z., Yumak, A., Badnell, N. R., Loch, S. D., & Pindzola, M. S. 2006, *A&A*, 447, 1165
- André, M. K., et al. 2003, *ApJ*, 591, 1000
- Asplund, M., Grevesse, N., & Sauval, A. J. 2005, in *ASP Conf. Ser. 336: Cosmic Abundances as Records of Stellar Evolution and Nucleosynthesis*, 25
- Blum, R. D. & Pradhan, A. K. 1992, *ApJS*, 80, 425
- Bruhweiler, F. C. 1984, in *Local Interstellar Medium*, ed. Y. Kondo, F. C. Bruhweiler, & B. D. Savage, 39–50
- Burgess, A. 1965, *ApJ*, 141, 1588
- Dupuis, J., Vennes, S., Bowyer, S., Pradhan, A. K., & Thejll, P. 1995, *ApJ*, 455, 574
- Frisch, P. C. & Slavin, J. D. 2003, *ApJ*, 594, 844
- Frisch, P. C. & Slavin, J. D. 2006, in *Solar Journey: The Significance of Our Galactic Environment for the Heliosphere and Earth*, editor P. C. Frisch (Springer), in press
- Frisch, P. C., et al. 1999, *ApJ*, 525, 492
- Genova, R., Beckman, J. E., Molaro, P., & Vladilo, G. 1990, *ApJ*, 355, 150
- Gloeckler, G. & Geiss, J. 2004, *Advances in Space Research*, 34, 53
- Gondhalekar, P. M., Phillips, A. P., & Wilson, R. 1980, *A&A*, 85, 272
- Grevesse, N. & Sauval, A. J. 1998, *Space Science Reviews*, 85, 161
- Gruen, E., Gustafson, B., Mann, I., Baguhl, M., Morfill, G. E., Staubach, P., Taylor, A., & Zook, H. A. 1994, *A&A*, 286, 915
- Gry, C. & Jenkins, E. B. 2001, *A&A*, 367, 617
- Gu, M. F. 2004, *ApJS*, 153, 389
- Hayes, M. A. & Nussbaumer, H. 1984, *A&A*, 134, 193
- Hébrard, G., Mallouris, C., Ferlet, R., Koester, D., Lemoine, M., Vidal-Madjar, A., & York, D. 1999, *A&A*, 350, 643
- Izmodenov, V., Malama, Y. G., Gloeckler, G., & Geiss, J. 2003, *ApJ*, 594, L59

- Jenkins, E. B., et al. 2000, *ApJ*, 538, L81
- Jura, M. 1974, *ApJ*, 191, 375
- Keenan, F. P., Lennon, D. J., Johnson, C. T., & Kingston, A. E. 1986, *MNRAS*, 220, 571
- Kingdon, J. B. & Ferland, G. J. 1996, *ApJS*, 106, 205
- Kruk, J. W., et al. 2002, *ApJS*, 140, 19
- Lallement, R. & Ferlet, R. 1997, *A&A*, 324, 1105
- Lehner, N., Jenkins, E., Gry, C., Moos, H., Chayer, P., & Lacour, S. 2003, *ApJ*, 595, 858
- Lyu, C. H. & Bruhweiler, F. C. 1996, *ApJ*, 459, 216
- Möbius, E., et al. 2004, *A&A*, 426, 897
- Mathis, J. S., Mezger, P. G., & Panagia, N. 1983, *A&A*, 128, 212
- McClintock, W., Henry, R. C., Linsky, J. L., & Moos, H. W. 1978, *ApJ*, 225, 465
- Nussbaumer, H. & Storey, P. J. 1986, *A&AS*, 64, 545
- Oliveira, C. M., Dupuis, J., Chayer, P., & Moos, H. W. 2005, *ApJ*, 625, 232
- Slavin, J. D. & Frisch, P. C. 2002, *ApJ*, 565, 364
- . 2006, *ApJ*, (in preparation)
- Spitzer, L. 1978, *Physical Processes in the Interstellar Medium* (New York: Wiley-Interscience, 1978)
- Field, G. B. & Steigman, G. 1971, *ApJ*, 166, 59
- Verner, D. A., Ferland, G. J., Korista, K. T., & Yakovlev, D. G. 1996, *ApJ*, 465, 487
- Welty, D. E., Hobbs, L. M., Lauroesch, J. T., Morton, D. C., Spitzer, L., & York, D. G. 1999, *ApJS*, 124, 465
- Wilson, N. J. & Bell, K. L. 2002, *MNRAS*, 337, 1027
- Witte, M. 2004, *A&A*, 426, 835
- Wolff, B., Koester, D., & Lallement, R. 1999, *A&A*, 346, 969
- Wood, B. E. & Linsky, J. L. 1997, *ApJ*, 474, L39
- Wood, B. E., Redfield, S., Linsky, J. L., & Sahu, M. S. 2002, *ApJ*, 581, 1168

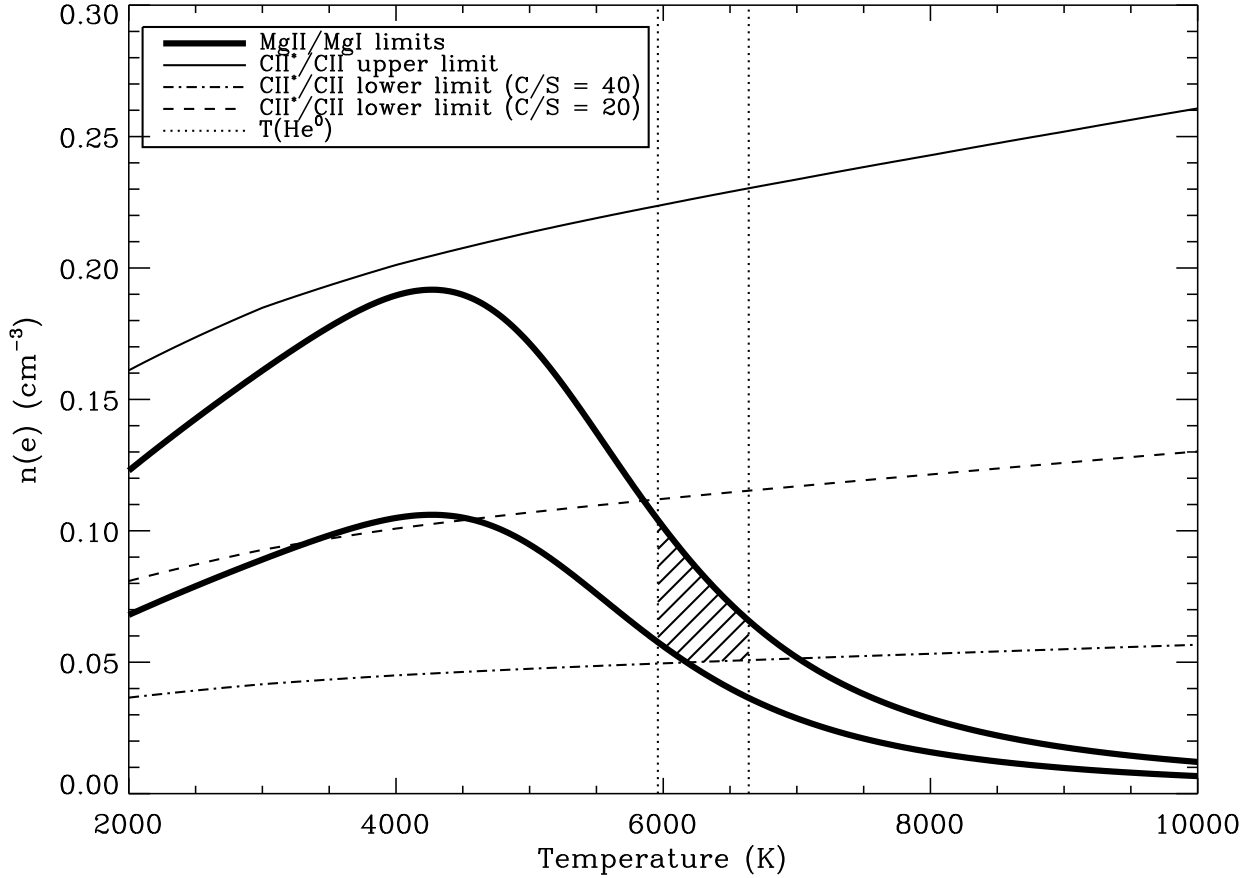


Fig. 1.— Constraints on the electron density and temperature in the LIC based on column density measurements towards ϵ CMa and *in situ* observations of the temperature. The thick lines show the constraints from the observations of Mg I and Mg II. The upper, thin solid line is the upper limit on the electron density using the lower limit on $N(\text{C II})$ derived directly from the observations. The dashed and dashed-dot lines show the lower limit on $n(e)$ that result from an upper limit on $N(\text{C II})$ under the assumptions of a C/S abundance ratio of 20 and 40 respectively. The vertical dotted lines indicate the temperature limits based on *in situ* observations of He^0 .

Table 1. Observational Constraints

Observed Quantity	Observed Value	Reference
$N(\text{C II})$ (cm^{-2})	$1.4 - 2.1 \times 10^{14}$	1
$N(\text{C II}^*)$ (cm^{-2})	$1.3 \pm 0.2 \times 10^{12}$	1
$N(\text{O I})$ (cm^{-2})	$1.4_{-0.2}^{+0.5} \times 10^{14}$	1
$N(\text{Mg I})$ (cm^{-2})	$7 \pm 2 \times 10^9$	1
$N(\text{Mg II})$ (cm^{-2})	$3.1 \pm 0.1 \times 10^{12}$	1
$N(\text{S II})$ (cm^{-2})	$8.6 \pm 2.1 \times 10^{12}$	1
$T(\text{K})$	6300 ± 340	2
$n(\text{He I})$ (cm^{-3})	0.015 ± 0.0015	2

References. — (1) Gry & Jenkins (2001) (Values shown are for the LIC component towards ϵ CMa, component 1.), (2) Witte (2004).